BOUNDARY ELEMENT METHOD ANALYSIS OF THERMOELASTIC DEFORMATION IN NONHOMOGENEOUS MEDIA

SOMNATH GHOSH and SUBRATA MUKHERJEE
Department of Theoretical and Applied Mechanics, Thurston Hall, Cornell University, Ithaca, NY 14853, U.S.A.

Abstract—This paper presents a boundary element method (BEM) formulation and numerical implementation of thermoelasticity problems in nonhomogeneous media. The formulation uses the known kernels of the displacement equations for elasticity problems in homogeneous media. This formulation leads to a domain integral containing the unknown displacement field in addition to the usual boundary integrals with displacements and tractions. An iterative scheme is used to determine the displacement fields.

Numerical results are presented for some illustrative plane strain problems. The iterative scheme is shown to converge rapidly for these problems with moderate temperature gradients. The BEM results are compared with results from the finite element method (FEM) for these problems, and also with exact solutions whenever possible.

INTRODUCTION

The subject of this paper is the solution of thermoelasticity problems in general nonhomogeneous media by the boundary element method (BEM). Such problems are of interest in many engineering applications where metallic components are loaded in the presence of thermal gradients. The most common reason for interest in nonhomogeneous media arises from the fact that material parameters such as the Young's modulus are temperature dependent. Thus, if such a dependence is included in the mathematical model, the material parameters become functions of temperature and hence of position within the body.

The corresponding problem in a homogeneous medium has been solved before by the BEM (see, e.g. Rizzo and Shippy[1]). In their paper, Rizzo and Shippy used the well known fundamental solutions of the Navier equations governing displacements in an elastic solid. Unfortunately, however, such fundamental solutions are not known, in general, for a nonhomogeneous medium. One possibility is to obtain a BEM formulation based on the fundamental solutions of the homogeneous medium problem, as has been suggested by Butterfield[2] for potential flow problems in nonhomogeneous bodies. This approach leads to a domain integral involving the unknown displacement field in addition to the usual boundary integrals. Such an approach has been adopted in this paper.

There have been some recent attempts by Tanaka and Tanaka[3, 4] to obtain integral formulations for heat conduction and thermoelasticity problems in nonhomogeneous media, but these papers are mathematical in nature and do not contain any numerical results. The present paper describes a BEM formulation and numerical implementation for plane strain thermoelasticity problems in nonhomogeneous media. Careful attention is paid to important practical questions such as accurate numerical evaluation of singular integrals and the development of an iterative algorithm for the calculation of the displacement field. While the mathematical formulation and numerical solution method are valid for problems involving general nonhomogeneous media, the numerical examples presented here are concerned with problems where the spatial dependence of the young's modulus arises from its dependence on temperature. The BEM numerical results for illustrative problems are compared with results from the finite element method (FEM) as well as with an exact solution which is available for a simple example. The efficiency and accuracy of the two methods—BEM and FEM—are compared in the context of solution of problems in nonhomogeneous media. Readers interested in the power and range of applicability of the BEM are referred to two recent books on the subject, one by Banerjee and Butterfield[5] and the other by Mukherjee[6].

GOVERNING EQUATIONS FOR PLANE STRAIN PROBLEMS

Navier equations for displacements

Plane strain problems are considered in this paper. The cross section of the body is assumed to lie in the x_1–x_2 plane and the displacement and strain components in the transverse direction, u_3 and ϵ_{33}, are taken to be zero. The first assumption made for this thermoelastic problem is that each component of the strain tensor ϵ_{ij} can be additively decomposed into an elastic and a thermal part $\epsilon_{ij}^{(e)}$ and $\epsilon_{ij}^{(T)}$, respectively. Thus,

$$\epsilon_{ij} = \epsilon_{ij}^{(e)} + \epsilon_{ij}^{(T)} = \epsilon_{ij}^{(e)} + \alpha T \delta_{ij} \tag{1}$$

where α is the coefficient of thermal expansion, T is the temperature (above some datum value) and δ_{ij} is the Kronecker delta. The range of indices in eqn (1) is $i = 1, 2; j = 1, 2$. It is also valid for the transverse direction, in which

$$\epsilon_{33} = \epsilon_{33}^{(e)} + \alpha T = 0. \tag{2}$$

The elastic strain tensor is related to the stress tensor σ_{ij} through the usual Hook's law. The stress tensor satisfies the equilibrium equations and the total strain is related to the displacements u_i through the usual kinematic relations

$$\epsilon_{ij} = \epsilon_{ij}^{(e)} + \epsilon_{ij}^{(T)} = \tfrac{1}{2}(u_{i,j} + u_{j,i}). \tag{3}$$

The range of indices in eqn (3) and subsequent equations is 1, 2.

The equations of equilibrium can be written in terms of displacements by combining them with the constitutive and kinematic equations. Assuming the Lame parameters λ and $\mu(= G)$ to be functions of the spatial coordinates, the resultant Navier equations for thermoelastic deformation in a nonhomogeneous medium are

$$Gu_{i,jj} + \frac{G}{1-2v} u_{k,ki} + \lambda_{,i}u_{k,k} + G_{,j}(u_{i,j} + u_{j,i}) = -F_i + 2G\left(\frac{1+v}{1-2v}\right)\alpha T_{,i} + \alpha T (3\lambda_{,i} + 2G_{,i}) \tag{4}$$

where the new symbols used are v, the Poisson's ratio and F_i, the components of the body force vector per unit volume.

The usual mechanical boundary conditions, e.g. displacements, tractions or combinations therof must be prescribed on the boundary ∂B of the body. The components of the traction vector τ_i at a point on the boundary ∂B are given by the equation

$$\tau_i = G\left[\left\{(u_{i,j} + u_{j,i})n_j + \frac{2v}{1-2v} u_{k,k} n_i\right\} - \frac{2(1+v)}{(1-2v)} \alpha T n_i\right] \tag{5}$$

where n_i are the components of the unit outward normal to ∂B at that point.

The temperature field must be obtained by solving the diffusion equation with the appropriate thermal boundary conditions. In this paper, a steady state temperature field is assumed to prevail, so that

$$\nabla^2 T = 0 \tag{6}$$

where ∇^2 is the Laplacian operator in the x_1–x_2 plane. The thermal problem is solved first and the temperature field is then input into eqns (4) and (5). The material parameters λ, G (and hence v) are either prescribed functions of position or of temperature. In either case, they are known as functions of the spatial coordinates once eqn (6), with its appropriate boundary conditions, has been solved.

Direct BEM formulation for displacements

A BEM formulation for the displacement field is obtained by following the method outlined by Butterfield[2] for potential flow problems in nonhomogeneous media. The

auxilliary solution chosen here is that for homogeneous, isotropic, linear elasticity [7], i.e.

$$u_i^* = U_{ij}e_j \qquad (7)$$

where u_i^* satisfies the equation

$$u_{i,jj}^* + \frac{1}{1-2v_0}u_{k,ki}^* = -\frac{\Delta(p,q)}{G_0}\delta_{ij}e_j. \qquad (8)$$

In the above v_0 and G_0 are base properties for the homogeneous problem, Δ is the Dirac delta function and e_j are unit orthogonal base vectors. The two point function U_{ij} is the displacement at a field point q in the i direction due to a unit load at a source point p in the j direction. The function U_{ij} for plane strain is available in many references (see, e.g. [5–7]). The components of the traction vector τ_i^* in the homogeneous elasticity problem are related to the gradients of the displacement field according to the equation

$$\tau_i^* = G_0\left[(u_{i,j}^* + u_{j,i}^*)n_j + \frac{2v_0}{1-2v_0}u_{k,k}^* n_i\right]. \qquad (9)$$

Multiplying both sides of eqn (4) by u_i^* and integrating over the domain B of the body results in the equation

$$\int_B u_i^*\left[Gu_{i,jj} + \frac{G}{1-2v}u_{k,ki} + \lambda_{,i}u_{k,k} + G_{,j}(u_{i,j} + u_{j,i})\right]\mathrm{d}A$$
$$= \int_B u_i^*\left[-F_i + 2G\frac{(1+v)}{(1-2v)}\alpha T_{,i} + \alpha T(3\lambda_{,i} + 2G_{,i})\right]\mathrm{d}A. \qquad (10)$$

Using the definitions of tractions in eqns (5) and (9), and the divergence theorem, eqn (10) can be reduced to the form

$$\frac{G(p)}{G_0}u_j(p) = \int_{\partial B}\left[U_{ij}(p, Q)\tau_i(Q) - \frac{G(Q)}{G_0}T_{ij}(p, Q)u_i(Q)\right]\mathrm{d}c_Q$$
$$+ \int_B [\{U_{ij,k}(p,q) + U_{kj,i}(p,q)\}G_{,k}(q) + U_{kj,i}(p,q)\lambda_{,j}(q)]u_i(q)\,\mathrm{d}A_q$$
$$+ \int_B \left[U_{ij}(p,q)F_i(q) + 2U_{ij,i}(p,q)G(q)\frac{(1+v(q))}{1-2v(q)}\alpha T(q)\right]\mathrm{d}A_q$$
$$- \int_B U_{kj,i}(p,q)\left[G(q)\left\{\frac{1}{1-2v(q)} - \frac{1}{1-2v_0}\right\}u_i(q)\right]_{,i}\mathrm{d}A_q \qquad (11)$$

where the two point function T_{ij} is the usual one for homogeneous elasticity (see, e.g. [5–7]), lower case letters p and q denote points inside the body B and capital letters P and Q denote points on the boundary ∂B. A comma denotes a derivative with respect to a field point and $\mathrm{d}c_Q$ and $\mathrm{d}A_q$ are boundary and area elements respectively.

Equation (11) is seen to contain the unknown displacement field inside two of the domain integrals in addition to being in the boundary integral in the usual way. This is a consequence of the fact that the known fundamental solutions for the elasticity problem in a homogeneous medium (rather than for the nonhomogeneous medium which are, in general, not known) have been used to derive eqn (11). A domain integral containing the unknown function also occurs in plasticity (see, e.g. [5]) and in viscoplasticity problems with large strains[8]. The presence of domain integrals containing the unknown displacement field in eqn (11) requires iterations in order to arrive at the solution. This has been done in order to obtain the numerical solutions presented later in this paper.

A major simplification in eqn (11) occurs if the Poisson's ratio is assumed to be a constant. This is justifiable in problems with temperature dependent elastic properties since

v is typically a weak function of temperature. Making this assumption with $v_0 = v$ and ignoring body forces, yields a simplified form of eqn (11)

$$\frac{G(p)}{G_0} u_j(p) = \int_{\partial B} \left[U_{ij}(p,Q)\tau_i(Q) - \frac{G(Q)}{G_0} T_{ij}(p,Q)u_i(Q) \right] dc_Q$$

$$+ \int_B \left[\{U_{ij,k}(p,q) + U_{kj,i}(p,q)\}G_{,k}(q) + \frac{2v}{1-2v} U_{kj,k}(p,q)G_{,i}(q) \right] u_i(q) \, dA_q$$

$$+ \int_B 2\frac{(1+v)}{(1-2v)} U_{ij,i}(p,q)\alpha G(q)T(q) \, dA_q. \tag{12}$$

It should be noted that if G does not vary in space, the first domain integral on the r.h.s. of eqn (12) drops out and the resulting equation reduces to that for the case of thermoelastic deformation in a homogeneous medium (see, e.g. [9]). Also, as expected, eqn (12) is independent of the particular choice of the base shear modulus G_0. This becomes obvious once the explicit forms of U_{ij} and T_{ij} are taken into account in eqn (12).

The boundary integral equation is obtained from eqn (12) in the usual way by taking the limit as an internal point p approaches a point P on ∂B. This gives the equation

$$\frac{G(P)}{G_0} c_{ij}(P)u_i(P) = \int_{\partial B} \left[U_{ij}(P, Q)\tau_i(Q) - \frac{G(Q)}{G_0} T_{ij}(P, Q)u_i(Q) \right] dc_Q$$

$$+ \int_B \left[\{U_{ij,k}(P,q) + U_{kj,i}(P,q)\}G_{,k}(q) + \frac{2v}{(1-2v)} U_{kj,k}(P,q)G_{,i}(q) \right]$$

$$\times u_i(q) \, dA_q + \int_B \frac{2(1+v)}{(1-2v)} U_{ij,i}(P,q) \alpha G(q)T(q) \, dA_q. \tag{13}$$

The tensor c_{ij} is a function of the local geometry and the location of P and is available in other publications (e.g. [6, 10]). If the boundary is locally smooth at P, $c_{ij} = (\frac{1}{2})\delta_{ij}$.

The numerical implementation of eqn (13), that has been used to solve (13) for the displacement field, is described in the next section of the paper.

Internal stresses

Once the displacement field has been obtained throughout the body, the displacement gradients must be obtained by differentiating the displacement field. The stresses can then be obtained from Hooke's law

$$\sigma_{ij} = G \left[u_{i,j} + u_{j,i} + \frac{2v}{1-2v} u_{k,k}\delta_{ij} - \frac{2(1+v)}{(1-2v)} \alpha T\delta_{ij} \right]. \tag{14}$$

The displacement gradients can be obtained by one of two methods.

Analytical differentiation. In this approach, eqn (12) is differentiated at an internal source point to give

$$\frac{G(p)}{G_0} u_{j,L}(p) = -\frac{G_{,L}}{G_0}(p)u_j(p) + \int_{\partial B} U_{ij,L}(p,Q)\tau_i(Q) \, dc_Q - \int_{\partial B} \frac{G(Q)}{G_0} T_{ij,L}(p,Q)u_i(Q) \, dc_Q$$

$$+ \frac{\partial}{\partial x_L} \int_B \left[\{U_{ij,k}(p,q) + U_{kj,i}(p,q)\}G_{,k}(q) + \frac{2v}{1-2v} U_{kj,k}(p,q)G_{,i}(q) \right]$$

$$\times u_i(q) \, dA_q + \frac{\partial}{\partial x_L} \int_B \frac{2(1+v)}{(1-2v)} U_{ij,i}(p,q)\alpha G(q) T(q) \, dA_q. \tag{15}$$

This approach has the advantage of delivering a continuous strain and stress field inside B. The difficulty in implementing this method arises from the fact that, since $U_{ij,k}$ has a $1/r$ singularity, the last two integrals must first be integrated analytically for an arbitrary

source point p and then differentiated at p. This approach has been implemented in [6] for problems where integrals of the type $\int_B U_{ij,k}(p,q)\,dA_q$ are involved. In this problem, however, the domain integrals also contain the shear modulus, unknown displacement field, temperature etc. The complicated nature of the domain integrals renders the analytical differentiation method difficult to implement in this problem.

Numerical differentiation. In this approach, the displacements are interpolated within each internal cell by suitable shape functions and then these shape functions are differentiated element wise to give the strains. This strategy, therefore, uses the BEM to determine displacements throughout the body and then a method analogous to the FEM to obtain the strains. This method can be easily implemented but has the disadvantages of allowing discontinuities in stresses at internal nodes and across inter-cell boundaries.

NUMERICAL IMPLEMENTATION OF BEM

Some of the details of the numerical implementation of the BEM equations are given in this section. Further details are available in the M.S. Thesis of Ghosh[11].

Discretized equations

The boundary of the body ∂B is discretized into N_s straight segments and the interior is discretized into n_i triangular cells. A discretized version of eqn (13) is written as

$$\frac{G(P_M)}{G_0} c_{ij}(P_M)u_i(P_M) = \sum_{N_s} \int_{\Delta c_N} U_{ij}(P_M,Q)\tau_i(Q)\,dc_Q - \sum_{N_s} \int_{\Delta c_N} T_{ij}(P_M,Q)\frac{G(Q)}{G_0}u_i(Q)\,dc_Q$$

$$+ \sum_{n_i} \int_{\Delta A_n} \{U_{ij,k}(P_M,q) + U_{kj,i}(P_M,q)\}G_{,k}(q)u_i(q)\,dA_q$$

$$+ \sum_{n_i} \int_{\Delta A_n} \frac{2v}{1-2v} U_{kj,k}(P_M,q)G_{,i}(q)u_i(q)\,dA_q$$

$$+ \sum_{n_i} \int_{\Delta A_n} \frac{2(1+v)}{(1-2v)} U_{ij,i}(P_M,q)\,\alpha\, G(q)T(q)\,dA_q \tag{16}$$

where P_M is a boundary point P that coincides with a node M.

The temperature field is first obtained on ∂B and in B by solving the steady heat equation by the BEM. Suitable shape functions must now be chosen for the tractions, displacements and temperatures on ∂B and in B. The traction and displacement components and the temperature are assumed to be piecewise linear on the boundary segments Δc_N. Double nodes are placed at corners in order to allow for jumps in normals or traction components across them.

The shear modulus is assumed to be a linear function of temperature

$$G = G_0(k_1 + k_2 T). \tag{17}$$

Experimental results[12] show that this is a fairly good assumption unless the temperature is very high. Of course, this assumption can be relaxed and G can be made a nonlinear function of temperature.

The displacements and temperature are assumed to be piecewise linear on the triangular internal cells ΔA_n with the sampling points placed at the vertices of each triangle. By virtue of eqn (17), the shear modulus becomes piecewise linear and the gradients of G become piecewise constant on the internal cells. The gradients of G could have been evaluated pointwise internally from the equation

$$G_{,i} = \frac{\partial G}{\partial T} T_{,i}. \tag{18}$$

In such a case, shape functions for temperatures on internal cells would become

unnecessary. This procedure would be more accurate than the one used here but would be much more expensive.

Evaluation of boundary integrals in eqn (16)

As mentioned before, the tractions, displacements and shear modulus are piecewise linear on straight boundary segments. Hence, Gu_i is piecewise quadratic on these segments. The boundary integrals are evaluated analytically. This involves integration of functions of the type

$$\int_{\Delta c} T_{ij}\, dc, \quad \int_{\Delta c} cT_{ij}\, dc, \quad \int_{\Delta c} c^2 T_{ij}\, dc$$

as well as

$$\int_{\Delta c} U_{ij}\, dc \quad \text{and} \quad \int_{\Delta c} cU_{ij}\, dc$$

where c is the distance measured along a boundary segment of length Δc. Analytical integration of singular kernels is the most accurate way to obtain these integrals and is recommended whenever possible. This has been done here and further details are available in [11].

Evaluation of area integrals in eqn (16)

The kernel $U_{ij,k}$ has a singularity of the type $1/r$. Thus, the three area integrals in eqn (16) must be determined with great care. Analytical integration is perhaps possible here but is cumbersome. Instead, accurate numerical schemes have been used. These are described below.

Regular integrals. If the source point lies outside the internal cell over which the integral has to be evaluated, the integrand is regular. In this case, Gaussian quadrature with seven Gauss points in each triangle has been used.

Singular integrals. If a source point lies on or inside an internal cell, the integrand is singular. The latter case can arise when the displacements are evaluated at internal points. In this case, an analytical transformation prior to Gaussian quadrature has proved to be very useful. This transformation has been described in detail in [6, 11, 13]. The integrals in the transformed (square) domains are evaluated with nine Gauss points per square.

Iterative scheme for displacements

Numerical discretization transforms eqn (16) into an algebraic system of the type

$$[A]\{u\} + [B]\{\tau\} = [C] + [D] \tag{19}$$

where the coefficient matrices $[A]$ and $[B]$ contain boundary integrals of the kernels, U_{ij}, etc. $[C]$ *represents the area integrals containing components of the unknown displacement field* and $[D]$ is obtained from the last (known) integral in eqn (16). The presence of u_i in the matrix $[C]$ requires iterations in order to solve eqn (19). This procedure is described below.

(a) The starting values of the internal displacements are taken to be zero. Equation (19), with $[C] = 0$, is solved for the unknown boundary components of the displacements and tractions in terms of the prescribed ones and the known matrix $[D]$. The matrix $[D]$ is only calculated once and remains invariant throughout the iterative process.

(b) With $[C]$ still equal to zero, the boundary values of $\{u\}$ and $\{\tau\}$ are used in a discretized version of eqn (12) to yield the first approximation to the internal displacement field.

(c) A first approximation to $[C]$ is obtained with the internal displacement field from step (b), and eqn (19) is solved again to obtain the second approximation to the boundary values of $\{u\}$ and $\{\tau\}$. All these quantities are then used in the discretized version of eqn (12) to yield the second approximation to $u_i(p)$.

(d) Step (c) is repeated as many times as necessary till convergence is achieved and the displacement field is known everywhere and the traction field is known on ∂B.

Evaluation of internal stresses

A finite element type approach has been used here to obtain the displacement gradients from the displacement field. The piecewise linear internal displacement field is differentiated to yield piecewise constant displacement gradients on the internal cells. The internal stresses are then obtained from eqn (14).

Evaluation of boundary stresses

The boundary stresses can be accurately determined from operations only on the boundary. Once the displacements and tractions are evaluated on the boundary, the tangential derivatives of the displacements, $(\partial u_i/\partial c)$, are obtained by differentiating the boundary shape functions. All the components of boundary stresses can now be obtained from the constitutive and stress–traction equations. Details of this procedure are available in [6, 11, 14].

THE STEADY STATE TEMPERATURE FIELD BY THE BEM

The uncoupled steady state temperature field throughout B and on ∂B must be obtained before the thermoelastic problem can be attempted. This is done here by solving Laplace's equation

$$\nabla^2 T = 0 \qquad (20)$$

by the BEM. The admissible boundary conditions are prescribed T, or $(\partial T/\partial n)$ or combinations thereof on the boundary ∂B of the body.

The BEM solution of this problem is obtained in standard fashion by the direct BEM method (see [5]). The boundary-integral equation, in this case, is

$$c(P)T(P) = \int_{\partial B} \left[E(P, Q)T(Q) - F(P, Q)\frac{\partial T}{\partial n}(Q) \right] dc_Q \qquad (21)$$

where the kernels are

$$E = \frac{1}{2\pi}\frac{\partial}{\partial n}(\ln r_{PQ}), \quad F = \frac{1}{2\pi}\ln r_{PQ}$$

where r_{PQ} is the distance between P and Q and $c = \hat{\alpha}/2\pi$, $\hat{\alpha}$ being the included angle at the corner at P.

As before, the boundary ∂B is discretized into N_s straight boundary elements. The temperature and its normal derivative are assumed to be piecewise linear on the boundary segments. Double nodes are placed at corners to allow for jumps in $(\partial T/\partial n)$ across them. The kernels are integrated analytically. The discretized version of eqn (21) is solved for the unspecified components of T and $(\partial T/\partial n)$ in terms of the prescribed ones. Once T and $(\partial T/\partial n)$ are known on ∂B, an equation analogous to (21) for an internal point p is used to obtain the temperature distribution throughout B. Further details of this procedure are available in [11].

THE FINITE ELEMENT METHOD

The BEM results for specific problems are compared with those obtained by the FEM. The FEM computer program that has been used here has been described earlier in [5]. Triangular finite elements are used in the program with piecewise quadratic displacements (LST) (as opposed to piecewise linear displacements in the BEM). Integrals over each element are carried out by Gaussian quadrature with seven Gauss points per element. The temperature dependent Young's modulus is taken to be piecewise constant over the finite elements.

NUMERICAL RESULTS FOR PLANE STRAIN PROBLEMS

Material parameters

The material parameters used in the numerical calculations are representative of 304 stainless steel. The parameters used are (see eqn (17))

$$G_0(\text{at } 25°C) = 11.54 \times 10^6 \text{ psi}$$

$$k_1 = 1.005 \qquad\qquad k_2 = -1.915 \times 10^{-4}°C^{-1}$$

$$v = 0.3 \qquad\qquad \alpha = 0.125 \times 10^{-4}°C^{-1}.$$

Problems considered

Two types of illustrative problems are considered in this paper. The first type is a square cross-section in plane strain subjected to a temperature gradient. This problem is solved by the BEM and FEM and these results are compared against an exact solution which can be obtained for this problem. The second class of problems is that of a thick cylinder subjected to a temperature gradient with and without internal pressure. The BEM and FEM results for displacements and stresses are compared with each other for these problems.

Square cross-section in plane strain

This is a simple problem in which a unit square cross-section is subjected to a temperature gradient in the x_2 direction and constrained in x_1 direction as shown in Fig. 1. The main reason for choosing this problem is computer code verification.
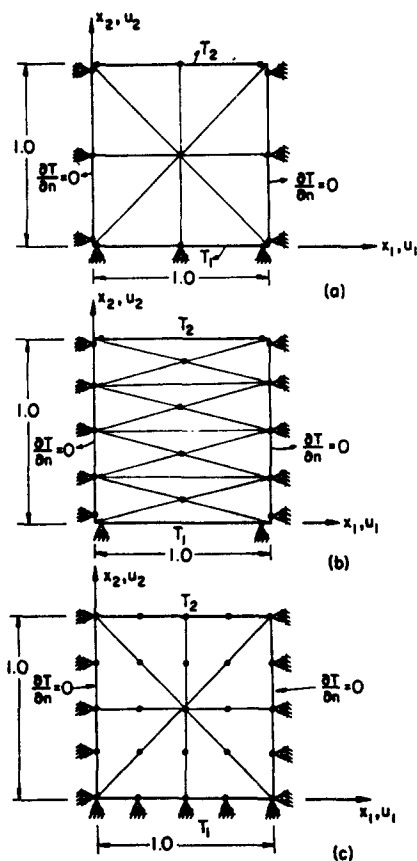

Fig. 1. Square cross-section subjected to a temperature variation along the x_2 direction and free to expand in x_2 direction only. (a) BEM mesh with 12 boundary nodes and 8 internal cells, (b) BEM mesh with 14 boundary nodes and 16 internal cells, (c) FEM mesh with 25 nodes and 8 elements.

An exact solution for this problem can be easily obtained as

$$T = (T_2 - T_1)x_2 + T_1$$

$$\sigma_{11} = \sigma_{33} = -2\alpha\frac{(1+\nu)}{(1-\nu)}GT$$

$$u_2 = \alpha\frac{(1+\nu)}{(1-\nu)}\left[\frac{(T_2-T_1)}{2}x_2{}^2 + T_1 x_2\right] \tag{22}$$

with all other components of stress and displacement equal to zero.

This problem has been solved with a coarse and a fine BEM mesh and a FEM mesh as shown in Fig. 1. The temperatures are taken as $T_1 = 30°C$ and $T_2 = 50°C$.

The results for displacements and stresses are tabulated in Tables 1 and 2, respectively.

Table 1. Displacement solutions (u_2) in (inches) in the x_2 direction for a nonhomogeneous square plate with $T_1 = 30°C$ and $T_2 = 50°C$.

POINT COORDINATE X_2	EXACT	BEM 12 B. NODES	BEM 14 B. NODES	FEM 8 ELEMENTS
(0.25)	0.188616×10^{-3}		0.188847×10^{-3}	0.1885971×10^{-3}
(0.5)	0.40625×10^{-3}	0.406988×10^{-3}	0.406792×10^{-3}	0.4062622×10^{-3}
(0.75)	0.65290×10^{-3}		0.653823×10^{-3}	0.6528919×10^{-3}
(1.0)	0.928571×10^{-3}	0.932055×10^{-3}	0.931055×10^{-3}	0.928474×10^{-3}
(0.125)	0.906808×10^{-4}		0.87158×10^{-4}	
(0.375)	0.293805×10^{-3}		0.294089×10^{-3}	
(0.625)	0.525948×10^{-3}		0.526798×10^{-3}	
(0.875)	0.7871094×10^{-3}		0.793902×10^{-3}	

Table 2. Stress (σ_{11}) distribution along the x_2 direction in (psi) for the nonhomogeneous square plate with $T_1 = 30°C$ and $T_2 = 50°C$.

POINT COORDINATE X_2	EXACT	BEM 12 B. NODES	BEM 14 B. NODES	FEM 8 ELEMENTS
0.04166	- 16469.938		- 16789.2	
0.125	- 17345.738		- 17329.80	
0.1666	- 17783.07	- 17033.3		- 17774.09
0.208333	- 18220.034		- 17869.4	
0.25	- 18656.625		- 18580.9	
0.29166	- 19092.84		- 18919.0	
0.3333	- 19528.86	- 20169.1		- 19537.64
0.375	- 19964.27		- 19942.8	
0.45833	- 20834.19		- 20964.7	
0.5	- 21268.55	- 21215.6	- 21242.4	
0.54166	- 21702.55		- 21494.2	
0.625	- 22569.43		- 22543.4	
0.6666	- 23002.508	- 22244.7		- 22990.55
0.7083	- 23435.02		- 23590.9	
0.75	- 23867.16		- 23907.1	
0.7916	- 24298.93		- 23328.7	
0.8333	- 24730.33	- 25262.5		- 24721.9
0.875	- 25161.361		- 25054.4	
0.9583	- 26022.52		- 26777.2	
1.0	- 26452.446	- 26168.2	- 26240.9	

The FEM results are virtually exact. The BEM results, particularly with the fine mesh, are also excellent, the maximum deviation from the exact solution being of the order of one percent for the displacement and two percent for the stress, with most of the results lying within about half a percent of the exact solution. The BEM solution converges rapidly within four of five iterations. It must be noted here that the BEM computer program uses piecewise linear displacements on boundary elements as well as on the internal cells, while the FEM uses piecewise quadratic displacements on the finite elements.

The thick cylinder

A thick cylinder in plane strain is considered here. The cylinder has inner and outer radii of 1 in. and 1.5 in., respectively. The inner curved surface is at a temperature T_1 and the outer one is at a temperature T_2. The lateral surfaces of the cylinder are insulated so that there is only a radial temperature gradient. The cylinder is subjected to an internal pressure p_i.

The BEM and FEM discretizations for the problems are shown in Fig. 2. The number of internal elements—40—is the same for both. The FEM mesh has 99 nodes while the BEM mesh has 22 boundary nodes (including four double nodes).

Thermal loading only. In these examples, $T_1 = 30°C$, $T_2 = 50°C$ or $200°C$ and $p_i = 0$. The displacements calculated from the two methods, as functions of radial location, are shown in Figs. 3 and 5 and the corresponding circumferential stresses are shown in Figs. 4 and 6, respectively. The traction results for $\sigma_{\theta\theta}$ in Figs. 4 and 6 are those obtained from the boundary tractions along the edge $x_2 = 0$ of the quarter cylinder (see Fig. 2). The stresses at the internal points are obtained by interpolating the displacements (from the BEM eqn (12)) on internal cells and then differentiating the shape functions for each element. These stresses are referred to as those obtained by the "mixed BEM" approach in Figs. 4 and 6. The displacement and stress results from the two methods are very close. The FEM
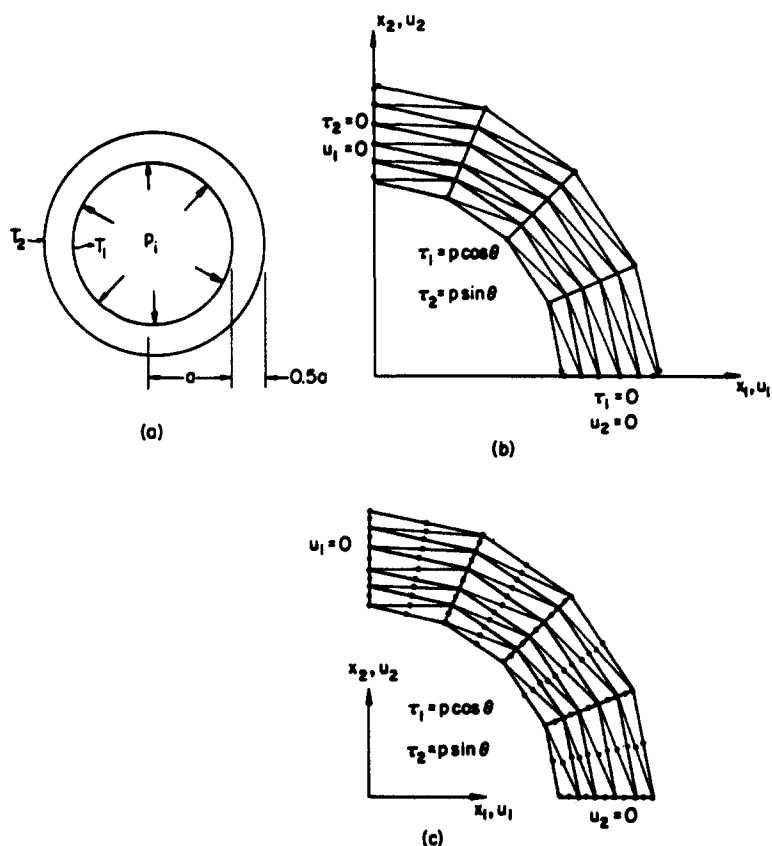

Fig. 2.(a) Thick cylinder with internal pressure and radial temperature distribution. (b) BEM mesh with 22 boundary nodes and 40 internal cells. (c) FEM mesh with 99 nodes and 40 elements.
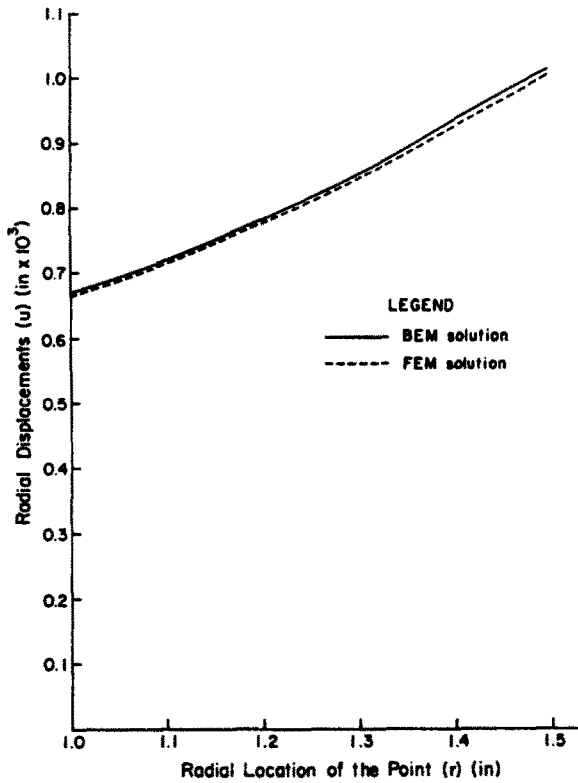
Fig. 3. Radial displacements in the nonhomogeneous cylinder with internal temperature $T_1 = 30°C$ and external temperature $T_2 = 50°C$.
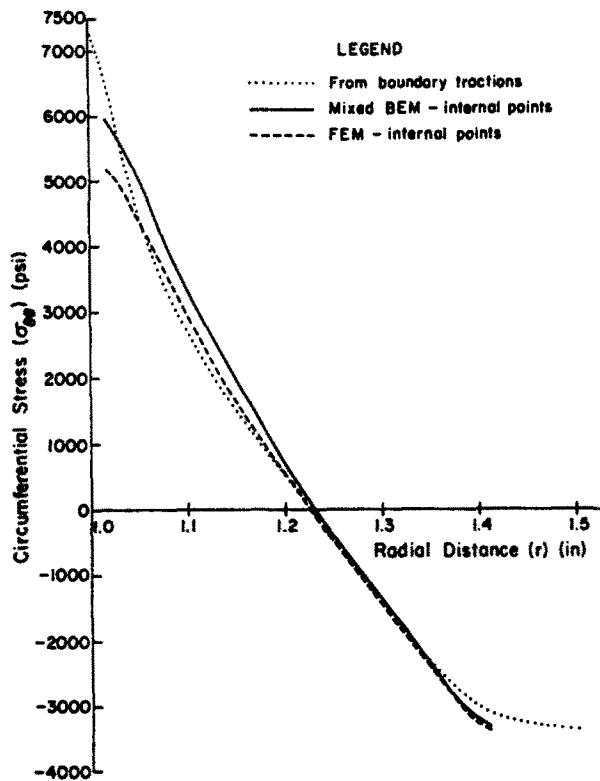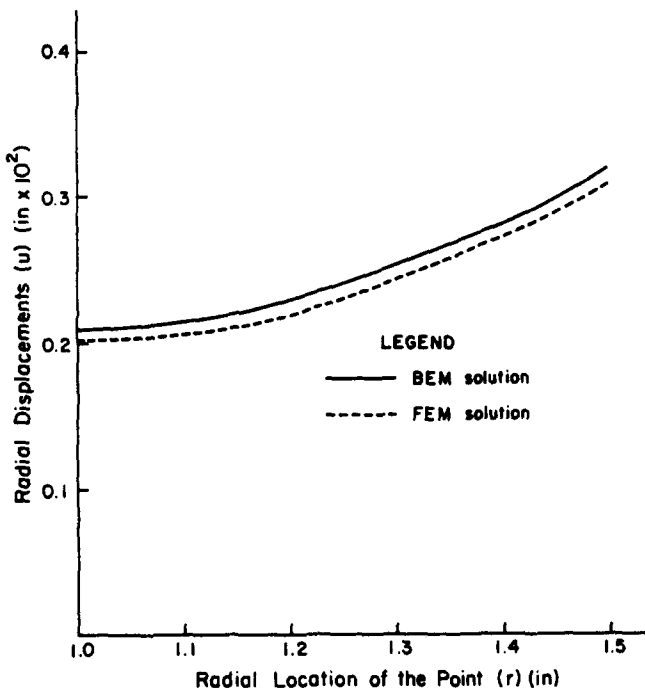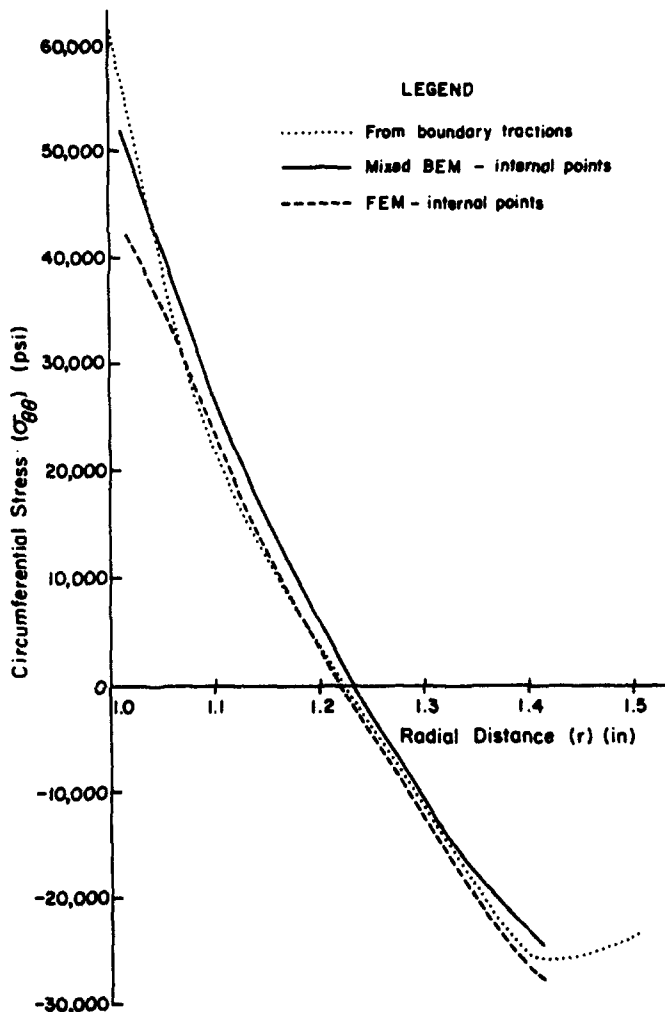

Fig. 4. Circumferential stresses in the nonhomogeneous cylinder with internal temperature $T_1 = 30°C$ and external temperature $T_2 = 50°C$.

Fig. 5. Radial displacements in the nonhomogeneous cylinder with internal temperature $T_1 = 30°C$ and external temperature $T_2 = 200°C$.

Fig. 6. Circumferential stresses in the nonhomogeneous cylinder with internal temperature $T_1 = 30°C$ and external temperature $T_2 = 200°C$.
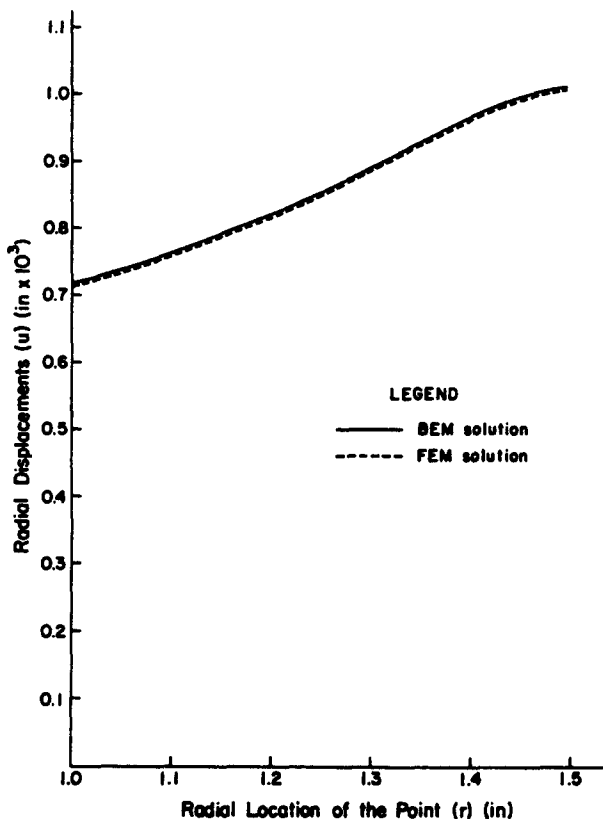
Fig. 7. Radial displacements in the nonhomogeneous cylinder with internal pressure $p_i = 500$ psi, internal temperature $T_1 = 30°C$ and external temperature $T_2 = 50°C$.
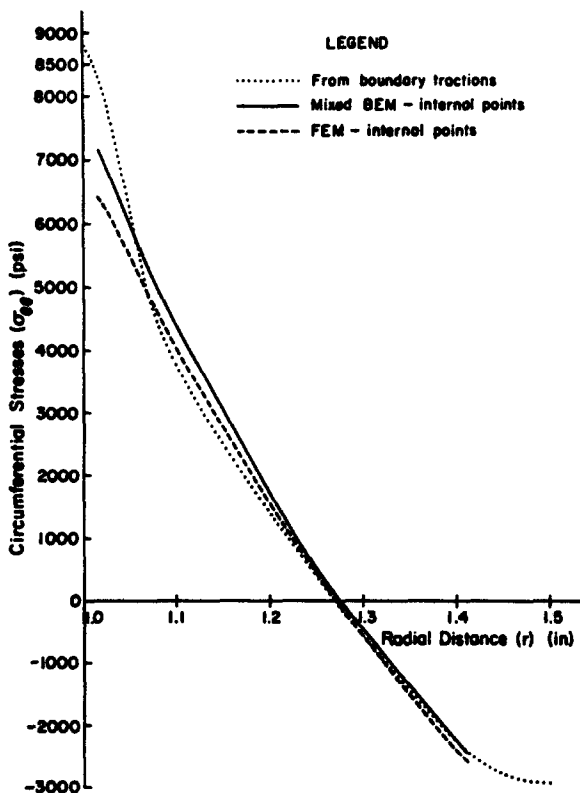

Fig. 8. Circumferential stresses in the nonhomogeneous cylinder with internal pressure $p_i = 500$ psi, internal temperature $T_1 = 30°C$ and external temperature $T_2 = 50°C$.

Table 3. Computation time comparison in (sec)

	BEM (12 Boundary Nodes)	BEM (14 Boundary Nodes)	FEM (8 Elements)
Square Plate	1.116	2.417	0.365

	BEM (22 Boundary Nodes)	FEM (40 Elements)
Cylinder with Thermal Loading Only ($T_1 = 30°$ C and $T_2 = 50°$ C)	10.01	2.814
Cylinder with Thermal Loading Only ($T_1 = 30°$ C and $T_2 = 200°$ C)	12.678	2.761
Cylinder with Thermal Loading and Internal Pressure	10.02	2.831

displacements are slightly lower than those from the BEM. A direct solution is not available for this problem.

Thermal and mechanical loadings. In this last example, $T_1 = 30°$C, $T_2 = 50°$C and $p_i = 500$ psi. Comparison of displacements and stresses from the two methods appears in Figs. 7 and 8, respectively. Once again, the displacements solutions are very close to each other and the stress solutions are quite close. The BEM displacement solutions again converge within a few iterations.

Computer times

The c.p.u. times on an IBM 370/168 for the above problems are given in Table 3. The FEM times are seen to be considerably less than the corresponding BEM times for this first BEM attempt.

DISCUSSION

This paper reports on part of a continuing research effort by Mukherjee and his co-workers at Cornell University aimed at critically evaluating the accuracy and efficiency of the BEM for a wide class of boundary value problems in solid mechanics. Previous publications have reported on BEM solutions to several elastic–viscoplastic problems relating to planar and axisymmetric deformation, torsion of bars, bending of plates as well as creep-fracture[6]. Recently, the BEM has been used to solve viscoplasticity problems in the presence of large strains and deformations [8] and a paper comparing the BEM and FEM for a simple boundary value problem for Laplace's equation is to be published soon [16]. This is a first attempt at solving thermoelasticity problems in nonhomogeneous media by the BEM.

The finite element method is a natural for nonhomogeneous problems since variational or Galerkin type formulations easily accomodate spatial variation of elastic properties. The BEM attempt here uses the kernels of the elasticity problem in a homogeneous medium to solve thermoelastic problems in a nonhomogeneous medium. This approach requires iterations in order to arrive at the displacement field. This BEM formulation is demonstrated to deliver accurate results for several sample problems within just a few iterations.

The computational effort for this first BEM attempt is seen to be larger than the corresponding FEM solutions. It is expected that the accuracy and efficiency of the BEM can be further improved if fundamental solutions for nonhomogeneous media become available. An algorithm to determine internal stresses pointwise by analytical differentiation of the displacement field should improve the accuracy of the BEM stresses. Finally, the BEM

computer times can possibly be improved by "fine tuning" of the existing first attempt BEM code.

REFERENCES

1. F. J. Rizzo and D. J. Shippy, An advanced boundary integral equation method for three-dimensional thermoelasticity. *Int. J. Num. Meth. Engng* **11**, 1753 (1971).
2. R. Butterfield, An application of the boundary element method to potential flow problems in generally inhomogeneous bodies. *Recent Advances in Boundary Element Method* (Edited by C. A. Brebbia), p. 123. Pentech. Press, London (1978).
3. M. Tanaka and K. Tanaka, Transient heat conduction problems in inhomogeneous media discretized by means of boundary volume element. *Nucl. Engng Des.* **60**, 381 (1980).
4. M. Tanaka and K. Tanaka, On numerical scheme for thermoelastic problems in inhomogeneous media by means of boundary volume element. *ZAMM* **60**, 719 (1980).
5. P. K. Banerjee and R. Butterfield, *Boundary Element Methods in Engineering Science.* McGraw Hill, New York (1981).
6. S. Mukherjee, *Boundary Element Methods in Creep and Fracture.* Applied Science Publishers (1982).
7. F. J. Rizzo, An integral equation approach to boundary value problems of classical elastostatics. *Qly. Appl. Math.* **25**, 83 (1967).
8. A. Chandra and S. Mukherjee, Boundary element formulations for large strain-large deformation problems of viscoplasticity. *Int. J. Solids Structures* (in press).
9. V. Kumar and S. Mukherjee, A boundary integral equation formulation for time-dependent inelastic deformation in metals. *Int. J. Mech. Sci.* **19**, 713 (1977).
10. P. C. Riccardella, *An implementation of the boundary-integral technique for planar problems of elasticity and elastoplasticity. Report No. SM*-73-10. Department of Mechanical Engineering, Carnegie Mellon University, Pittsburgh, PA (1973).
11. S. Ghosh, *Thermoelastic analysis of plane strain problems by the boundary element method.* M.S. Thesis, Department of Theoretical and Applied Mechanics, Cornell University, Ithaca, NY (1982).
12. R. H. Tien and O. Richmond, Theory of maximum tensile stresses in the solidifying shell of a constrained rectangular casting. *ASME J. Appl. Mech.* **49**, 481 (1982).
13. V. Sarihan and S. Mukherjee, Axisymmetric viscoplastic deformations by the boundary element method. *Int. J. Solids Structures* **18**, 113 (1982).
14. F. J. Rizzo and D. J. Shippy, A formulation and solution procedure for the general nonhomogeneous elastic inclusion problem. *Int. J. Solids Structures* **4**, 1161 (1968).
15. M. Morjaria and S. Mukherjee, Finite element analysis of time-dependent inelastic deformation in the presence of transient thermal stresses. *Int. J. Num. Meth. Engng* **17**, 909 (1981).
16. S. Mukherjee and M. Morjaria, On the efficiency and accuracy of the boundary element method and the finite element method. *Int. J. Num. Meth. Engng* (in press).